Ocean Sci. Discuss., 12, 2535–2564, 2015
www.ocean-sci-discuss.net/12/2535/2015/
doi:10.5194/osd-12-2535-2015

Ocean Science Discussions
Open Access

Seasonal hydrography and surface outflow in a fjord with deep sill: the Reloncavi fjord, Chile

M. I. Castillo[1,2], U. Cifuentes[2,6], O. Pizarro[2,3,4], L. Djurfeldt[5], and M. Caceres[1]

[1]Facultad de Ciencias del Mar y de Recursos Naturales,
Universidad de Valparaíso, Valparaíso, Chile
[2]Center for Oceanographic Research in the Eastern South Pacific (COPAS)-Sur Austral,
Universidad de Concepción, Concepción, Chile
[3]Departamento de Geofísica, Universidad de Concepción, Concepción, Chile
[4]Instituto Milenio de Oceanografía, Universidad de Concepción, Chile
[5]Department of Oceanography, Earth Sciences Center,
Gothenburg University, Gothenburg, Sweden
[6]Departamento de Oceanografía y Medio Ambiente, Instituto de
Fomento Pesquero, Valparaíso, Chile

Received: 19 September 2015 – Accepted: 9 October 2015 – Published: 29 October 2015

Correspondence to: M. I. Castillo (manuel.castillo@uv.cl)

Published by Copernicus Publications on behalf of the European Geosciences Union.

Abstract

Seasonal information of temperature, salinity, dissolved oxygen (DO) and chlorophyll, combined with meteorological and river discharge time series were used to describe the oceanographic conditions in the Reloncavi fjord (41°35′ S; 72°20′ W). The winds in the fjord valley blow mainly down-fjord during winter, reinforcing the upper layer outflow, while in spring–summer winds have a predominant up-fjord direction contrary to upper layer outflow. The fjord, with a deep sill at the mouth, was well stratified year-round and showed a thin surface layer of brackish water with mean salinities between 10.4 ± 1.4 (spring) and 13.2 ± 2.5 (autumn). The depth of the upper layer changed slightly along the different studied seasons remaining at about 4.5 m near the mouth. This upper layer presented a mean outflow (Q_1) of $3185 \pm 223\,\mathrm{m^3\,s^{-1}}$, which imply a flushing time of about 3 days of this layer. The vertical salt flux was ~ 37 tons of salt per second, similar to the horizontal salt flux observed in the upper layer. These estimations will contribute to a better management of the aquaculture on this region.

1 Introduction

The fjords are narrow coastal inlets generally deep due to advance and retrieve of glaciers (Stigebrandt, 2012). The study of these areas has been widely reported for the Scandinavian and North East Pacific fjords (Farmer and Freeland, 1983; Inall and Gillibrand, 2010), but little is known about the physical dynamics of one of world's most extensive fjords region: the austral Chilean fjords (Silva and Palma, 2008; Pantoja et al., 2011; Iriarte et al., 2014).

The austral Chilean fjord area extended from 41.5 to 55.9° S which is about 1700 km of fjords (~ 40 % of the total length of Chile) an area about $2.4 \times 10^5\,\mathrm{km^2}$ (Silva et al., 2011). Since early 80's the region between 41.5–42° S, has been intensively used for fish, shellfish and seaweed productions. In these days, the southern limit of the aquaculture is around 46° S and there are plans to cover until the 55° S in

2015 (http://www.subpesca.cl). Most of the Chilean aquaculture production comes from salmon farms which has become the fourth largest economic activity of Chile (Buschman et al., 2009). Despite the high utilization of fjords, the knowledge of the physical dynamics remains understudied. In fact, in the Chilean fjord region there are limited environmental data available in both space and time (e.g. Silva and Palma, 2008). As an example, there is only preliminary knowledge (e.g. Davila et al., 2002) about the impact on Chilean Patagonia circulation of the freshwater supply in a region with high river discharge (Niemeyer and Cereceda, 1984).

One of the first fjords used for salmon aquaculture in Chile was the Reloncavi fjord (centered at 41.5° S, 72.5° W). Even though this is one of the most studied fjords in southern Chile, oceanographic information is relatively scarce and several questions about its natural and anthropogenic variability remain unanswered. Soto and Norambuena (2004) pointed out the concern about the impact of the aquaculture on the system. As an example, Valle-Levinson et al. (2007) found lower (but over critical levels) dissolved oxygen (DO) concentration ($> 2\,\mathrm{mL\,L^{-1}}$) near the fjord's head, but its variability and impact on the biology along the seasons remain unknown. In addition, in this region León-Muñoz et al. (2013) indicated the existence a significant association between the increase of surface salinity and low DO concentrations, but the variability and relationship between these parameters below 2 m depth remain unknown. Montero et al. (2011) made along-fjord observations which were focused on seasonal variability of primary production. They did not observe DO as low as Valle-Levinson et al. (2007) thus, a detailed DO description is needed.

The mean circulation in the RF indicated that along-fjord currents had a three-layer vertical pattern: a thin (< 5 m) outflow upper layer, a thick intermediate inflow layer (> 5 and < 100 m) and a weak deep (> 100 m) outflow layer (Valle-Levinson et al., 2007; Castillo et al., 2012). This 3-layer pattern could be an important structure but only sporadically observed because it will be masked by wind forcing, remote forcing and freshwater pulses (Valle-Levinson et al., 2014).

OSD
12, 2535–2564, 2015

Despite the diverse studies made in the Reloncavi fjord, many questions remain unanswered about its hydrographic conditions and circulation, for example the seasonal variability of the salinity and the exchanges with the area outside the fjord. Here we present a study of the hydrographic seasonality and salinity fluxes using an extensive and high quality data set.

2 Study area

The Reloncavi Fjord (RF) has an overall length is 55 km and the averaged width of 2.8 km (Table 1) its waters are directly connected to Reloncavi Sound and indirectly to Ancud Gulf which is connected to Pacific Ocean through the Chacao channel (at the north of Chiloe Island) and by the Corcovado Gulf (Fig. 1). There is a deep-sill (∼ 200 m depth) located at 15 km from the mouth, this structure does not seem to be a barrier to the exchange of properties with external waters. The fjord has four sub-basins: (I) mouth-Marimeli, (II) Marimeli-Puelo, (III) Puelo-Cochamo and (IV) Cochamo-Petrohue. The mean depths of each sub-basins are 440, 250, 200 and 82 m, respectively (Fig. 1).

The main fresh water input to RF is trough the Puelo River, located at the center of the fjord, with annual discharge of 650 $m^3 s^{-1}$. Another important freshwater supply (annual mean of 255 $m^3 s^{-1}$) is the Petrohue River (located at the head). Minor freshwater inputs are associated to the Cochamo River (annual mean of 20 $m^3 s^{-1}$) (Niemeyer and Cereceda, 1984) and from Canutillar hydroelectric plant (75.5 $m^3 s^{-1}$ annual mean) (Fig. 1). The fresh water input due to direct precipitation on the fjord is only about 2 % of the main rivers discharge (León-Muñoz, 2013) and for the water and salt balances made in this study its contribution was considered balanced by evaporation.

Winds in the region had large seasonal variability. North and northwest winds are predominating during autumn–winter, while south and southwest winds prevail during spring–summer (Saavedra et al., 2010). Seasonal changes of the wind pattern were associated with an abrupt austral winter–spring transition observed in the temperature of the surface layer in the RF (Montero et al., 2010). During winter, the along-fjord wind

Discussion Paper | Discussion Paper | Discussion Paper | Discussion Paper |
OSD
12, 2535–2564, 2015
Seasonal hydrography in the Reloncavi fjord, Chile
M. I. Castillo et al.

stress (τ_y) is mainly out of fjord with intensities $< 0.2\,\mathrm{N\,m^{-2}}$. In summer, τ_y is directed into the fjord, opposing the surface outflow, with intensities between 0.1 and $0.3\,\mathrm{N\,m^{-2}}$. Additionally, during this season τ_y had a clear diurnal cycle (Montero et al., 2011) probably related to the radiational tide effect (Farmer and Freeland, 1983; Rabinovich and Medvedev, 2015).

Currents have a 3-layer pattern near the mouth. The thin upper outflow was relatively faster reaching $30\,\mathrm{cm\,s^{-1}}$ near the surface. Below that layer exists an intermediate inflow which never exceeds $10\,\mathrm{cm\,s^{-1}}$. The deep layer is thick and weak $\sim 1\,\mathrm{cm\,s^{-1}}$ this third layer has been suggested as a consequence of a tidal rectification of the flow (Valle-Levinson et al., 2007) and recently has been studied in detail for different fjords of southern Chile (Valle-Levinson et al., 2014). This pattern could change seasonally between a 2-layered during winter to 3-layered flows during spring–summer.

Additionally, there are evidences of an internal oscillation with a period of about 3 days (Castillo et al., 2012). One of the most recently study on this region (León et al., 2013) found a significant association between the temporal increase of near surface (1.5 m depth) salinity with lower surface DO concentrations, however their observations not describe the vertical structures or distribution of each parameters within the fjord. The objectives of this study were study and describe the seasonality of the hydrography of the Reloncavi fjord and to make estimations of the upper flow to obtain reliable flushing times estimations.

3 Data and methods

3.1 Discharge, meteorological, hydrographic (CTD) and current (ADCP) measurements

Except for the ADCP current time series, most data were registered in all seasons. The representative months for each season used in this study were: September to November for spring, December to February for summer, March to May for autumn and June

OSD
12, 2535–2564, 2015

to August for winter. A right-handed coordinate system was used for currents and surface wind stress vectors, where z is positive upward and the along-fjord (y component) was positive toward the fjord head. Consequently, the cross-fjord x component was positive toward east at the head and toward the south at the mouth.

The data of the Puelo River discharge were provided by Direccion General de Aguas, Chile (www.dga.cl). The data is regularly collected in a station located 12 km up-stream of the Puelo River's mouth (Fig. 1) and extended from January 2003 to December 2011. Here gaps represented ~ 2 % of the total. Although the discharge of the Petrohue River (RPt) was not directly measured an estimation of its runoff was obtained using Puelo River (RP) discharge throughout a linear regression between both annual cycles. In the case of the RP the annual cycle was estimated with data between 1975 and 1981 while the annual cycle of the RPt was based on the period 1941–1982 (Niemeyer and Cereceda, 1984). Both annual cycles were highly correlated ($R^2 = 0.88$) then $\mathrm{RPt} = 0.519 \times \mathrm{RP} - 68.173$. Due to the lack of data during the study period, the discharge of the Cochamo River ($20\,\mathrm{m^3\,s^{-1}}$) and from the Canutillar hydroelectric ($75.5\,\mathrm{m^3\,s^{-1}}$) were considered as constant supplies (Niemeyer and Cereceda, 1984; Sistema Interconectado Central, Chile,www.cdec-sic.cl).

A meteorological station was installed near the Puelo River mouth (see Fig. 1). The station included sensors for wind direction and magnitude (here wind directions are referred to by the direction from which the wind comes according to meteorological convention), solar radiation, rain and air temperature. The wind magnitude and direction sensors were installed 10 m over the sea-level and were set to collect data every 10 min from 12 June 2008 to 30 March 2011, here gaps represented only 0.04 %. Wind stress (τ) was calculated using a drag coefficient which depend of magnitudes (see Large and Pond, 1981) and a constant air density of $1.2\,\mathrm{kg\,m^{-3}}$.

The hydrographic data were collected using a CTD SeaBird 25 equipped with a SeaBird 43 dissolved oxygen sensor and a Wet-Lab/Wet-Star fluorometer (ECO-AFL). The concentration of chlorophyll a ($\mathrm{mg\,m^{-3}}$) from Fluorescence was accordingly to the relation provided by the CTD manufacturer. The CTD-Oxygen/Fluorometer

OSD
12, 2535–2564, 2015

(CTDOF) measurements were conducted in 19 along the fjord stations (Fig. 1). The CTD were conducted in transects which took between 12 and 18 h in 7 August 2008 (winter), 9 November 2008 (spring), 6 February 2009 (summer) and 9 June 2009 (autumn). In the case of winter measurements only reached ~ 50 m depth due to problems with the oceanographic winch. During those casts the CTD was not equipped with oxygen sensor.

Current measurements were made using Acoustic Doppler Currentmeter Profilers (ADCPs). Near the fjord's mouth a mooring with two ADCPs were installed. The mooring included a 75 kHz ADCP located near the bottom (450 m depth) and a 300 kHz ADCP located at 10 m depth. Another mooring with a 300 kHz at 15 m depth was installed near of Cochamo. The objective for installing the 300 kHz ADCP at ~ 10 m depth was to obtain good velocity measurements near the surface. The instruments in both systems were programmed to measure every 10 min in depth cells of 1 m. The depth of reference for velocity profiles were the surface. Currents were decomposed in along-fjord (v) and cross-fjord (u) component using a right-handed coordinate system as mentioned above. To focusing on the sub-tidal and sub-inertial variability, the along-fjord wind stress (τ_y) and currents (u, v) were filtered using a Cosine–Lanczos low-pass filter with half-amplitude of 40 h.

The upper volume flux (Q_1) was estimated using the velocity profiles at the mouth and Cochamo (Fig. 1). The Q_1 was estimated according to,

$$Q_1 = b \int_{z=0}^{z=v_0} v \mathrm{d}z \tag{1}$$

here, b is the fjord width near the surface at the mooring location (b was considered constant, despite sea level may change around 6 m during spring tides), v is the along-fjord velocity which change with depth z. The integration was made between the surface ($z = 0$) and the depth where v is zero ($z = v_0$). The use of up-looking ADCPs implies a lack of about 6 % (1 m for both ADCPs) of range due to side lobe effect. To

OSD
12, 2535–2564, 2015

estimate v until surface two methods of extrapolation were used: linear and nearest in a similar way used by Kirincich et al. (2005). Note that negative (positive) values of τ_y and v indicate out of (into) the fjord directions. Similar interpretation must be done with Q_1.

Associated to the estimation of Q_1 is possible to obtain the flushing time of the upper layer (F_{t1}) if the total volume of the upper layer (V_1) is introduced, thus $F_{t1} = V_1 Q_1^{-1}$. Additionally, if the upper mean Salinity (S_1) is considered, it is possible to estimate the horizontal salt flux $\mathrm{Fs_h} = Q_1 S_1$.

The $\mathrm{Fs_h}$ was compared with the total vertical salt flux ($\mathrm{Fs_T}$) at the base of the surface layer. To obtain $\mathrm{Fs_T}$ it is necessary obtain the vertical salt flux ($\mathrm{Fs_v}$), which was estimated from $\mathrm{Fs_v} = \kappa_z \partial S/\partial z$. Here, the eddy diffusivity (κ_z) was estimated using the eddy viscosity (A_z) based on the relation suggested by Pacanowski and Philander (1981) where $A_z = 0.01(1+5\mathrm{Ri})^{-2} + 10^{-4}$ and $\kappa_z = A_z\ (1+5\mathrm{Ri})^{-1} + 10^{-5}$. Here $\mathrm{Ri} = N^2/(\partial v/\partial z)^2$ is the Richardson number which was obtained from direct measurements of buoyancy frequency (N^2) and vertical shear of the along-fjord currents ($\partial v/\partial z$). The $\mathrm{Fs_T}$ was estimated introducing the surface horizontal area (A_h) at the mean depth of the upper layer thus $\mathrm{Fs_T} = \mathrm{Fs_v} A_\mathrm{h}$.

4 Results

4.1 Meteorological conditions and fresh water supply

The direction of winds had a marked dominance of the southeast and south, which represented up to 20 % during spring, summer and autumn. On the other hand, northerlies winds were dominant (c.a. 30 %) during winter. The maximum winds (> 10 m s^{-1}) were south and southeast during spring and summer (Fig. 2).

The seasonal variability of the daily cycle (in local-time) of the air temperature (°C), solar radiation (W m^{-2}), wind stress (N m^{-2}) and wind vector (m s^{-1}) was also analyzed (Fig. 3). The amplitude of the daily cycle for all variables was smaller during winter

OSD
12, 2535–2564, 2015

(June–September) and larger during the spring–summer (November–February). The air temperature had narrow range (between 6–8 °C) in winter compared with summer (12–18 °C). The solar radiation clearly had daylight variability (longer in summer than winter). Similar pattern were observed on air temperature and wind stress (τ) magnitude. In winter the amplitude of the daily cycle of τ was nearly zero, while during spring–summer maximum values of τ were observed between 3 p.m. and 6 p.m. local time.

The freshwater supply due to river discharges in the RF had maximum during June (winter) where the mean discharge was $1400 \pm 400\,m^3\,s^{-1}$. Typically on this region, rivers have a secondary maximum associated to the spring–summer snow melting which was observed in November ($1300 \pm 300\,m^3\,s^{-1}$). Lower river discharges were observed during late summer (February–March) and were lower than the annual mean of Puelo River ($< 650\,m^3\,s^{-1}$).

4.2 Seasonal hydrography: along-fjord CTD measurements.

Based on the depth of the 24 and 31 isohalines, three layers were defined to describe the hydrographic conditions in the RF. The upper layer was defined between the surface and the 24 isohaline depths (ih24) which coincide with the depth of the maximum gradient of salinity along-fjord. The rate of increasing density with depth throughout this upper layer was rather constant, without a clear mixing layer. The mean temperatures in this layer was 8.68 ± 0.32 °C during winter and 17.79 ± 0.37 °C during summer. Furthermore, mean salinities were 10.43 ± 1.36 during spring and 13.18 ± 2.47 during autumn. Additionally, the pycnocline depth at the fjord's mouth was observed at 1.7 m during winter and at 2.9 m during summer. Near the fjord's head the pycnocline reached a maximum depth of 8 m during winter. Seasonal changes of the mean depth of the pycnocline for the entire fjord were small, it changed from 4.05 ± 0.41 m in autumn to 4.79 ± 0.53 m during spring (Table 2). This suggests that the fjord maintains the stratification of the upper layer along the different seasons even with significant changes in the river discharges and winds (Figs. 4 and 6).

OSD
12, 2535–2564, 2015
Seasonal hydrography in the Reloncavi fjord, Chile
M. I. Castillo et al.

The 31 isohaline (ih31) represent the upper limit for the Modified Subantarctic Water (MSAAW) located in the inland sea outside the RF (Silva and Palma, 2008). The intermediate layer (depths between ih24 and ih31) had mean temperatures ranged between $10.22 \pm 0.14\,^{\circ}\mathrm{C}$ (winter) and $15.29 \pm 0.48\,^{\circ}\mathrm{C}$ (summer) consistent with high radiation of summer. The mean salinities ranged between 28.98 ± 0.46 in autumn to 29.61 ± 0.37 in winter. In addition, the mean depth of ih31 shoaling from 10.97 ± 2.49 m during spring to 7.96 ± 0.84 m during autumn suggesting that waters during autumn were more saline than other seasons (Fig. 4).

Slight changes in both, temperature and salinity were observed in the deep layer (depths > ih32), there observed temperatures changed between $10.61 \pm 0.05\,^{\circ}\mathrm{C}$ (winter) to $10.96 \pm 0.12\,^{\circ}\mathrm{C}$ (autumn), whereas salinities changed from 32.27 ± 0.16 (winter) to 32.68 ± 0.16 (autumn), which was consistent with the presence of more saline waters during autumn.

In general, surface waters in the Reloncavi fjord are over saturated with oxygen (DO > 6 $\mathrm{mL\,L^{-1}}$) during spring and summer, whereas in autumn and winter DO decreases. Oversaturated waters were observed between 1 to 15 m depth in spring and between 2 to 10 m depth during summer here DO was as high as 10 $\mathrm{mL\,L^{-1}}$ at the sub-basins III and IV near of the head (Fig. 5). In addition, waters with DO < 3 $\mathrm{mL\,L^{-1}}$ (~ 50 % saturation) were observed near the bottom in sub-basin III during spring. These waters occupied a more extended area in the fjord basin during summer and autumn. Waters with DO < 2.5 $\mathrm{mL\,L^{-1}}$ were observed near the bottom of sub-basins III and IV during summer and autumn.

The surface concentration of chlorophyll *a* (chl *a*) was extremely low during winter (slightly major than 0 $\mathrm{mg\,m^{-3}}$) and no major changes occur along the seasons. In general, fjord's waters registered chl *a* < 6 $\mathrm{mg\,m^{-3}}$ during winter, spring and autumn and were especially low chl *a* (~ 1 $\mathrm{mg\,m^{-3}}$) during winter. The exception was observed during summer in waters between 3 and 12 m depths, where chl *a*, was as high as 25 $\mathrm{mg\,m^{-3}}$ along the entire fjord. An interesting feature was observed at the entrance

OSD
12, 2535–2564, 2015

of sub-basin IV where this high concentration had a disruption probably due to changes in depth and width of the fjord at that region (Fig. 5).

4.3 Variability of the upper flow

In the period between 8 August to 9 November 2008, the filtered time series of Puelo river discharge, along-fjord wind stress (τ_y) and upper flows were compared (Fig. 6).

The Puelo river discharge had two contrasting periods: the first at the end of August (winter) with high discharge (> $10^3\,m^3\,s^{-1}$) this change the second week of September (spring) where the discharge was maintained between 500 and 650 $m^3\,s^{-1}$ (Fig. 6a). Similarly, τ_y pattern change from negative during winter, to positive during spring. This is a seasonal change from winter to spring conditions which also could be maintained during summer (see Castillo et al., 2012). In general, $|\tau_y|$ was $< 3 \times 10^{-2}\,N\,m^{-2}$. There were three events which that intensity was exceeded: in 11 and 15 August, and 16 September in all those cases τ_y blow towards the fjord's head (Fig. 6b).

Using the subtidal current profiles, the upper flow were estimated taken a width (b) of 2.9 km at the mouth, and 1.3 km at Cochamo. The time series of volume flux (Q_1) estimated with a nearest extrapolation sub-estimate in about 8 % compares the linear extrapolation. Note that all the results and discussion are based on the linear extrapolation.

At Cochamo during the end of winter Q_1 tend to be higher than during early spring. The inflows were observed only during spring, in all those cases $Q_1 < 10^3\,m^3\,s^{-1}$, for instance Q_1 average was $-583.31 \pm 446.43\,m^3\,s^{-1}$. Additionally, Q_1 had oscillations of about 2–3 days which are not present in the river discharge or wind-stress time series (Fig. 6d).

During the end of winter the outflow reached peaks larger than $7.5 \times 10^3\,m^3\,s^{-1}$ at the mouth, here Q_1 tend to reduce toward spring and rarely exceeded $5 \times 10^3\,m^3\,s^{-1}$. There were intense inflows events ($\sim 2.5 \times 10^3\,m^3\,s^{-1}$) which also were highly related with winds events (in the same direction) with intensities of about $2 \times 10^{-2}\,N\,m^2$. A crosscorrelation analysis between τ_y and Q_1 at the mouth indicated a maxima coefficient of correlation of 0.7 with 4 h lag, which implies a significant relation between the wind stress and the upper flow. Similarly to Cochamo, Q_1 time series had 3 days oscillations, these oscillations seems to be more evident during the early spring (Fig. 6c).

It is of interest to make a comparison between winter and spring using the mean velocity profiles and flows for each period. During the end of winter, winds were out of fjord (mean wind stress of $-0.3 \pm 7 \times 10^{-2}$ N m^{-2}) in the same direction of the upper current with intensities larger than 50 cm s^{-1}. Here Q_1 had a mean depth of 5.31 m. During winter the mean Q_1 was as high as -4045 ± 283 m^3 s^{-1} (outflow) which was ~ 3 times larger than the input of fresh water (R) into the fjord (Fig. 7a).

In early spring, τ_y was opposite (on average) to the upper currents (which were into the fjord) with a mean intensity of $1.1 \pm 5 \times 10^{-2}$ N m^{-2}, which was about 4 times greater than winter. Probably these opposite winds reduce the surface outflow which never exceeded 30 cm s^{-1} during this period. In addition, during spring the outflow was about half (-2050 ± 143 m^3 s^{-1}) the outflow observed in winter and nearly half of R (Fig. 7b).

Combining the observed Q_1 and typical salinity of the upper layer during winter and spring, it was possible to obtain the horizontal salt flux by the upper layer (Fs_h). In winter, Q_1 was 4045 m^3 s^{-1} and mean salinity (S_1) was 12.9 kg of salt per cubic meter (kg salt m^{-3}), taking a density (ρ_1) of 1009.8 kg m^{-3} for the upper layer. Thus, the total supply of salt by the upper layer during this season was $Fs_h = 52.3$ tons of salt per second (salt s^{-1}). During spring, upper salinity was 10.5 kg salt m^{-3} ($\rho_1 = 1007.6$ kg m^{-3}) and Q_1 was 2050 m^3 s^{-1} which imply a total supply of salt of $Fs_h = 21.5$ tons of salt s^{-1} during this season. Probably minor Fs_h during spring (compared with winter) were related to the high outflow and discharge differences in both seasons. A representative mean of Fs_h for the entire period could be obtained from Fs_h average of winter and spring which was 36.9 tons of salt s^{-1}.

OSD
12, 2535–2564, 2015

To estimate the vertical salt flux (Fs_v), the maximum N^2 and maximum $\partial v/\partial z$ were considered. In winter, Ri was 4.0 ($\kappa_z = 1.6 \times 10^{-5}\,m^2\,s^{-1}$) whereas in spring Ri was 36.2 ($\kappa_z = 1.1 \times 10^{-5}\,m^2\,s^{-1}$). In addition, maximum $\partial S/\partial z$ were 17.4 kg of salt m^{-4} in winter and 18.2 kg of salt m^{-4} in spring. The vertical salt flux (Fs_v) was 2.8×10^{-4} kg of salt $m^{-2}\,s^{-1}$ during winter and 1.9×10^{-4} kg of salt $m^{-2}\,s^{-1}$ during spring. Taking a typical salt flux of, 2.3×10^{-4} kg of salt $m^{-2}\,s^{-1}$. The total salt flux (Fs_T) to the upper layer could be estimated assuming that Fs_v is maintained over the horizontal Area (A_h) at 5 m depth (which is the deeper limit for the outflow, see Fig. 7), here $A_h = 1.59 \times 10^8\,m^2$ thus $Fs_T = 3.7 \times 10^4$ kg of salt s^{-1} or 37 tons of salt s^{-1}.

5 Discussion

A particular feature of the Reloncavi fjord is the deep sill located at about 13 km from the mouth (Fig. 1d). Usually, in fjords with deep or without sill the interior density distribution and variability is closely related with the outside stratification (e.g. Pedersen,1978). The earliest efforts to describe the Reloncavi fjord were summarized by Basten and Clement (1999),but their results are based on relatively few and sparse observations that preclude an adequate description of the seasonal variability.

5.1 Seasonality of the hydrography and freshwater inputs

To describe the seasonal conditions observed in the Reloncavi fjord, it is necessary describe the outer conditions on the region. In the Pacific Ocean in front of the Chiloe island (~ 42.5° S, 74° W), the water masses distribution indicate the presence of the Subantarctic Water (SAAW) in the first 100 m (salinity > 33) from the coast and further off shore (2000 km), below SAAW and nearshore (> 10 km) the Equatorial Subsurface Water (ESSW) it is perceptible until 350 m (Silva et al., 2009). Only those water masses could penetrate by the Guafo mouth and occupied the inland sea of Chiloe (Fig. 1). Here the presence of several island, sills and constrictions between the Corcovado

OSD
12, 2535–2564, 2015

and Ancud gulfs enhance turbulent mixing in the region. The mixing between SAAW and freshwaters produce a water masses with salinities between 31 and 33 as Modified Subantarctic Water (MSAAW) (Silva and Palma, 2008). The MSAAW occupied most of the interior basins of the Chilean fjord region (Perez-Santos et al., 2014). In summer, when river discharge is limited, surface salinities higher than 33 are present off the Guafo channel (Palma et al., 2011). In winter, coastal temperature and salinity in the Chilean fjord region seems to be controlled by the freshwater inputs (Davila et al., 2002).

The seasonal variability of winds in the Reloncavi fjord valley was consistent with the regional pattern observed in the south-central Chilean coast with southerlies winds during spring–summer and northerlies during autumn-winter periods (e.g. Saavedra et al., 2010). During spring and summer, the alongshore winds stress promote the upwelling near the coast (Strub et al., 1998; Sobarzo et al., 2007) in this process saltier deep water could reach the upper layer changing the near-shore hydrography.

This is also true for the Reloncavi fjord which had lower salinities and temperatures during winter (Fig. 4) when discharge present a relatively long term mean (eight years) of 1300 $m^3 s^{-1}$ (Fig. 2). It is worth noting that highest salinities (> 33) in the Reloncavi fjord were observed during autumn at the bottom of sub-basin I. In addition, these waters present relatively high temperatures ($\sim 11\,^{\circ}C$) and low DO (Figs. 4 and 5). These results suggest that denser ocean waters may reach the Reloncavi sound in fall. Nevertheless, based on limited data used in this study, it is not possible to know if this is a typical feature of the seasonal cycle.

According with this classification, the waters in the Reloncavi fjord are dominated along the seasons by EW in the upper layer and MSAAW in the deep layer (Fig. 4). Recent studies had reported the presence of MSAAW at Puyuhuapi (44.6° S, 72.8° W) fjord (Schneider et al.,2014) and into the Martinez channel (47.8° S, 73.7° W) in the southern Patagonia (Perez-Santos et al., 2014).

In the Reloncavi fjord, there is an unique connection (at the mouth) with the outer conditions and its deep sill (at 12 km from the mouth) seems not to be a barrier for

OSD
12, 2535–2564, 2015

the intrusion of MSAAW waters which could be maxima during autumn (Fig. 4 and 5). These also contribute to the propagation of remotely low-frequency oscillations to the interior of the Reloncavi fjord, which has been suggested as the forcing to 15 days oscillations observed in deep along-fjord currents (Castillo et al., 2012).

5.2 Reloncavi fjord exchanges

One important parameter in estuarine environments is the renewal capacity of the system. Unfortunately, the ADCP measurements do not covered the entire depths of the fjord basin to obtain a complete profile of the exchanges at the mouth. However, using the shallower ADCPs was possible to obtain reliable estimations of the surface outflow in this location (Fig. 6).

The wind stress variability was highly correlated ($r^2 = 0.7$) with the outflow at the mouth. During winter τ_y was negative in the same direction of the upper flow, thus τ_y may enhance the estuarine circulation. The surface outflow estuarine circulation seems to be sustained even during the spring with τ_y blowing against the upper flow. This is different to other estuarine system like the Juan de Fuca strait where the estuarine flow tends to switch between estuarine and transient flows due to the local wind influence (Thomson et al., 2007). In the Reloncavi fjord, an along-fjord wind stress $\tau_y \geq 3 \times 10^{-2} N\,\mathrm{m}^{-2}$ are able to balance the typical along-fjord pressure gradient (Castillo et al., 2012) and produce the observed inflows of the upper layer (Fig. 6b and c).

The estimations of the volume fluxes could help to obtain a first approximation of the water exchanges in the Reloncavi fjord. At the mouth, the average of the volume flux (Q_1) estimated from direct observations was $3185 \pm 223\,\mathrm{m}^3\,\mathrm{s}^{-1}$. One interesting (an operational) parameter is the flushing time of the upper layer (F_{t1}) which is determined by $F_{t1} = V_1 Q_1^{-1}$, where V_1 is the upper layer volume which is $8.30 \times 10^8\,\mathrm{m}^3$. The flushing time of the upper layer (F_{t1}) was 3 days, highly consistent with the period of the oscillations observed in the time series at the mouth and Cochamo (Fig. 6).

OSD
12, 2535–2564, 2015

The period of 3 days is also consistent with the natural period of oscillation of the fjord (internal seiche oscillations) reported by Castillo et al. (2012) and are mainly dominated by the first baroclinic mode (Castillo et al., in review). These oscillations probably play a role in the internal mixing of the fjord similarly to the Gullmard fjord (Arneborg and Liljebladh, 2001) where 36 % of the mixing is caused by the internal seiche. Additionally, this flushing time is the same order than the F_t estimated by Calvete and Sobarzo (2011) for the Aysen fjord (45°16′ S, 73°18′ W) nevertheless their results were based on the fresh water fraction using a thick upper layer of 20 m for all calculations contrary to this study where the upper layer depth had been determined by the isohaline of 24 depth (ih24). These flushing times estimations contrast with the 100 days estimated by Valle-Levinson et al. (2007) for the Reloncavi fjord basin but those estimation were made based on cross-fjord transects (measured on 1 day) of towed ADCP near of the Puelo River (in the center of the fjord). Here time series of Q_1 consider two months of velocity profiles obtaining the first reliable estimations of the upper flow for the Reloncavi fjord. In any case, these estimations must be taken carefully and in order to enlarge the results to the fjord basin future modeling studies must be made to obtain the residence times of any properties in the fjord.

The mean outflow at the mouth ($3185\,m^3\,s^{-1}$) was ~ 6 times the mean outflow at Cochamo ($583\,m^3\,s^{-1}$). The outflow at Cochamo represents the volume flux of sub-basin IV (near the fjord's head) which is dominated by the Petrohue river (Fig. 1). Taking an estimation of the Petrohue river of $318\,m^3\,s^{-1}$. Here the ratio R/Q_1 was 0.55 which imply that the outflow at Cochamo is nearly twice the freshwater input on this sub-basin.

Another way to obtain estimations of the exchanges is use the Knudsen's relations for a two-layered model. This method has been used to estimate the exchange flows in the Chilean fjords (e.g. Valle-Levinson et al., 2007; Calvete and Sobarzo, 2011). Although the use of this relation requires that the salinity to be in steady state which is only valid for long time scales (Geyer, 2010). In that case, the volume flux of the upper layer is defined by $Q_1 = Rf^{-1}$. Here, $f = (S_2 - S_1)/S_2$ is the fraction of freshwater (e.g.

Dyer, 1997) and R is the freshwater input to the fjord. Taking into account the salinity of winter f was 0.6 whereas in spring f was 0.68. The outflow estimated using the Knudsen relation during winter (spring) at the mouth was 2293 $m^3 s^{-1}$ (1403 $m^3 s^{-1}$). Notice that in both seasons the outflows were sub-estimated. They were ~ 2 times smaller than the values obtained using the mean observed flow, which imply longer flushing times than observed at the mouth. In contrary, at Cochamo (sub-basin IV) the freshwater fraction ($f = R/Q_1$) was 0.58, similar to the observed fraction of the sub-basin I.

These results suggest that the estimations of the water renewal of the upper layer using Knudsen's relation could be only valid on the sub-basin IV (upper part of the fjord) but not for the entire fjord. This could have significant implications for the management for the salmonids aquaculture in the region because the salmon cages generally occupied the first 20 m depth of the water column (Oppedal et al., 2011).

An interesting result was obtained from the estimations of the horizontal and vertical salt fluxes for the upper layer for the period between late winter to early spring (Fig. 6). The results indicate that ~ 37 tons of salt s^{-1} outflows from the upper layer and the same amount of salt is supply to the upper layer by the turbulent mixing (Fig. 7). These results suggest that the lower layer is able to sustain the output of salt from the upper layer maintaining (in a nearly) steady state of the amount of salt in the fjord. These results must be take carefully and probably requires more attention in future observational and numerical models studies on this region.

6 Conclusions

Winds in the region were consistent with the seasonal regional pattern, northerlies during winter and southerlies during summer. The maximum winds (> 10 $m s^{-1}$) were south and southeast in the afternoon of spring and summer. The freshwater supply had two maximums along the year, the principal was observed in winter

OSD
12, 2535–2564, 2015

($1400 \pm 400\,m^3\,s^{-1}$) during the pluvial season while the secondary was observed in spring ($1300 \pm 300\,m^3\,s^{-1}$) produced by the snow melting.

The pattern of the hydrography had marked seasonal changes. The waters during winter were colder than summer. In the upper 10 m depth, temperatures were nearly 8 °C whereas in summer it can reach 18 °C. The dissolved oxygen concentration (DO) of the Reloncavi fjord was higher than $2\,mL\,L^{-1}$ in all the seasons. The lowest DO was present during spring and autumn in sub-basin IV near the fjord's head.

The upper layer salinities (S_1) and densities (ρ_1) were lower during spring and higher during autumn. The change of the along-fjord pycnocline depth was minima which suggest that the stratification was maintained along the seasons. Although, minimum changes on salinity was observed on the deep layer this was consistent with more saline waters during autumn. This suggesting the intrusion of Subantarctic waters modified by mixing processes outside the fjord.

The mean Q_1 at the mouth was $3185 \pm 223\,m^3\,s^{-1}$ which was ~ 6 times the outflow of Cochamo ($583\,m^3\,s^{-1}$). At the mouth the results showed high differences between the estimated volume flux from the Knudsen' relation and the observed outflow, whereas at Cochamo the Knudsen's relation could be appropriated to estimate the volume flux of the sub-basin IV.

In the period between late winter and early spring, the upper layer had a flushing time of 3 days highly consistent with the natural internal period of the fjord.

The horizontal and vertical salt fluxes were highly consistent in the period between late winter and early spring. An amount of ~ 37 tons of salt per second supply to the upper layer this amount of salt was highly consistent with the output of salt by the upper layer.

Acknowledgements. The authors want to thank to several graduate students from the University of Gothenburg, Sweden, and undergraduate and graduate students from the University of Concepción (UdeC), Chile which collaborated in the fieldwork. This study is part of the PFB/31 COPAS-Sur Austral program and Centro de Investigación en Ecosistemas de la Patagonia trough FIP2007-21. M. I. Castillo was supported by FONDECYT grant #3130639.

References

Arneborg, L. and Liljebladh, B.: The internal seiches in Gullmar fjord part II – contribution to basin water mixing, J. Phys. Oceanogr., 31, 2567–2574, 2001.

Bastén, J. and Clement, A.: Oceanografía del estuario de Reloncaví, X región de Chile, Ciencia y Tecnologia del Mar, 22, 31–46, 1999.

Buschmann, A. H., Cabello, F., Young, K., Carvajal, J., Varela, D. A., and Henriquez, L.: Salmon aquaculture and coastal ecosystem health in Chile: analysis of regulations, environmental impacts and bioremediation systems, Ocean Coast. Manage., 52, 243–249, 2009.

Calvete, C., and Sobarzo, M.: Quantification of the surface brackish water layer and frontal zones in southern Chilean fjords between Boca del Guafo (43°30′ S) and Estero Elefantes (46°30′ S), Cont. Shelf. Res., 31, 162–171, 2011.

Castillo, M. I., Pizarro, O., Cifuentes, U., Ramirez, N., and Djurfeldt, L.: Subtidal dynamics in a deep fjord of southern Chile, Cont. Shelf. Res., 49, 73–89, 2012.

Dávila, P. M., Figueroa, D., and Müller, E.: Freshwater input into the coastal ocean and its relation with the salinity distribution off austral Chile (35–55° S), Cont. Shelf. Res., 22, 521–534, 2002.

Farmer, D. M. and Freeland, H. J.: The physical oceanography of Fjords, Prog. Oceanogr., 12, 147–194, 1983.

Geyer, W. R.: Estuarine salinity structure and circulation, in: Contemporary Issues in Estuarine Physics, edited by: Valle-Levinson, A., Cambridge Univ. Press, Cambridge, UK, 12–26, 2010.

Iriarte, J. L., Pantoja, S., and Daneri, G.: Oceanographic processes in Chilean fjords of Patagonia: From small to large-scale studies, Prog. Oceanogr., 129, 1–7, 2014.

Kirincich, A., Barth, J. A., Graham, B., Menge, B. A., and Lubchenco, J.: Wind-driven inner-shelf circulation off central Oregon during summer, J. Geophys. Res., 110, C10S03, doi:10.1029/2004JC002611, 2005.

Large, W. G. and Pond, S.: Open-ocean momentum flux measurements in moderate to strong winds, J. Phys. Oceanogr., 11, 324–336, 1981.

Leon-Muñoz, J., Marcé, R., and Iriarte, J. L.: Influence of hydrological regime of an Andean river on salinity, temperature and oxygen in a Patagonia fjord, Chile. New Zeal. J. Mar. Fresh., 47, 515–528, 2013.

Discussion Paper | Discussion Paper | Discussion Paper | Discussion Paper |

OSD

12, 2535–2564, 2015

Seasonal hydrography in the Reloncavi fjord, Chile

M. I. Castillo et al.

Montero, P., Daneri, G., González, H. E., Iriarte, J. L., Tapia, F. J., Lizárraga, L., Sanchez, N., and Pizarro, O.: Seasonal variability of primary production in a fjord ecosystem of the Chilean Patagonia: implications for the transfer of carbon within pelagic food webs, Cont. Shelf. Res., 31, 202–215, 2011.

Niemeyer, H. and Cereceda, P.: Hidrografía, Geografía de Chile. Instituto Geográfico Militar, Santiago, Chile, 313 pp., 1984.

Oppedal, F., Dempster T., and Stien, L. H.: Environmental drivers of Atlantic salmon behavior in sea-cages: a review, Aquaculture, 311, 1–18, 2011.

Pacanowski, R. C. and Philander, S. G. H.: Parameterization of vertical mixing in numerical models of the tropical oceans, J. Phys. Oceanogr., 11, 1443–1451, 1981.

Palma, S., Silva, N., C. Retamal, M., and Castro, L.: Seasonal and vertical distributional patterns of siphonophores and medusae in the Chiloe Interior Sea, Chile. Cont. Shelf. Res., 31, 260–271, 2011.

Pantoja, S., Luis Iriarte, J., and Daneri, G.: Oceanography of the Chilean Patagonia, Cont. Shelf. Res., 31, 149–153, 2011.

Pedersen, B.: A brief review of present theories of fjord dynamics, in: Hydrodynamics of Estuaries and Fjords, Elsevier Oceanography Series, edited by: Nihoul, J. J., 407–422, 1978.

Pérez-Santos, I., Garcés-Vargas, J., Schneider, W., Ross, L., Parra, S., and Valle-Levinson, A.: Double-diffusive layering and mixing in Patagonian fjords, Prog. Oceanogr., 129, 35–49, 2014.

Rabinovich, A. B. and Medvedev, I. P.: Radiational tides at the southeastern coast of the Baltic Sea. Oceanology, 55, 319–326, 2015.

Saavedra, N., Müller, E., and Fopiano, A.: On the climatology of surface wind direction frequencies for the central Chilean coast, Australian Meterological and Oceanographic Journal, 60, 103–112, 2010.

Schneider, W., Pérez-Santos, I., Ross, L., Bravo, L., Seguel, R., and Hernández, F.: On the hydrography of Puyuhuapi Channel, Chilean Patagonia. Prog. Oceanogr., 129, 8–18, 2014.

Silva, N. and Palma, S.: The CIMAR Program in the austral Chilean channels and fjords, in: Progress in the Oceanographic Knowledge of Chilean Inner Waters, From Puerto Montt to Cape Horn, edited by: Silva, N. and Palma, S., Comite Oceanográfico Nacional – Pontificia Universidad Católica de Valparaíso, Valparaíso, Chile, 11–15, 2008.

OSD
12, 2535–2564, 2015

Silva, N., Haro, J., and Prego, R.: Metals background and enrichment in the Chiloe Interior Sea sediments (Chile). Is there any segregation between fjords, channels and sounds?, Estuar. Coast. Shelf S., 82, 469–476, 2009.

Silva, N., Vargas, C. A., and Prego, R.: Land-ocean distribution of allochthonous organic matter in surface sediments of the Chiloe and Aysen interior seas (Chilean Northern Patagonia), Cont. Shelf. Res., 31, 330–339, 2011.

Sobarzo, M., Bravo, L., Donoso, D., Garcés-Vargas, J., and Schneider, W.: Coastal upwelling and seasonal cycles that influence the water column over the continental shelf off central Chile, Prog. Oceanogr., 75, 363–382, 2007.

Soto, D. and Norambuena, F.: Evaluation of salmon farming effects on marine systems in the inner seas of southern Chile: a large-scale mensurative experiment, J. Appl. Ichthyol., 20, 493–501, 2004.

Stigebrandt, A.: Hydrodynamics and circulation of fjords, in: Encyclopedia of Lakes and Reservoirs, edited by: Bengtsson, L., Herschy, R., and Fairbridge, R., Springer, Dordrecht, the Netherlands, 327–344, 2012.

Strub, P. T., Mesías, J. M., Montecino, V., Rutlant, J., and Salinas, S.: Coastal ocean circulation off western South America., in: The Sea, edited by: Robinson, A. R. and Brink, K. H., John Wiley & Sons, New York, USA, 273–313, 1998.

Thomson, R. E., Mihály, S. F., and Kulikov, E. A.: Estuarine vs. transient flow regimes in Juan de Fuca Strait, J. Geophys. Res.-Oceans, 112, C09022, doi:10.1029/2006JC003925, 2007.

Valle-Levinson, A., Sarkar, N., Sanay, R., Soto, D., and León, J.: Spatial structure of hydrography and flow in a Chilean fjord, Estuario Reloncaví, Estuar. Coast., 30, 113–126, 2007.

Valle-Levinson, A., Caceres, M., and Pizarro, O.: Variations of tidally driven three-layer residual circulation in fjords, Ocean Dynam., 64, 459–469, 2014.

OSD

12, 2535–2564, 2015

Table 1. Topographical features of sub-basins in the Reloncavi Fjord (RF). Here *b* is the width, *L* represent the length, *z* the depth.

Sub-basin	*b* (km)	*L* (km)	*z* (m)
I	2.2–4.5	14	400–460
II	2.3–4.2	15	140–280
III	3	16	180–200
IV	1.1–1.6	10	35–110
RF mean	2.8	55	250

OSD
12, 2535–2564, 2015

Table 2. Seasonal statistics of the mean depth of the upper layer, and densities of the upper and deep layers.

	h_1 [m]	ρ_1 [kg m^{-3}]	ρ_2 [kg m^{-3}]
Aug	4.60 ± 0.60	1009.72 ± 4.32	1024.62 ± 0.74
Nov	4.79 ± 0.53	1007.63 ± 5.32	1024.78 ± 0.62
Feb	4.68 ± 0.26	1008.77 ± 3.26	1024.78 ± 0.63
Jun	4.05 ± 0.41	1009.90 ± 3.92	1024.95 ± 0.48

OSD
12, 2535–2564, 2015

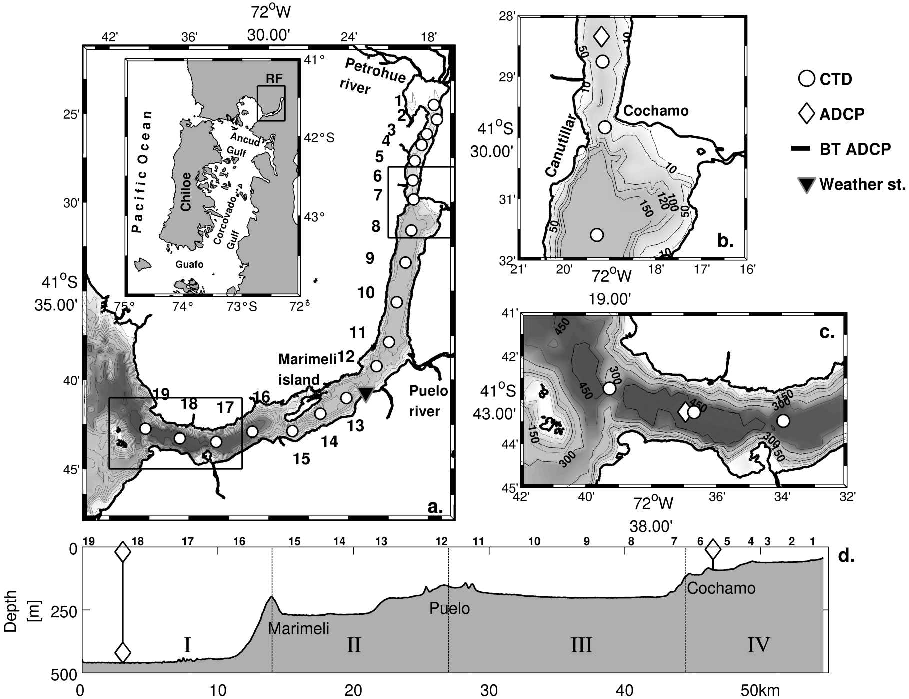

Figure 1. (a) The Reloncavi fjord region, and location of the instruments. The upper left insert shows the general region. The ADCP moorings are near the mouth (ADCP). The black lines indicate the underway ADCP (BT ADCP) transects. On the right, the inserts shows **(b)** the Cochamo and **(c)** the mouth regions. The lower insert **(d)** shows the along-fjord bathymetry, here the segmented lines indicate the sub-basins limits: mouth-Marimeli (I), Marimeli-Puelo (II), Puelo-Cochamo (III) and Cochamo-Petrohue (IV). The diamonds represent the location and depths of the ADCP mooring showed in **(c)**.

OSD
12, 2535–2564, 2015

Seasonal hydrography in the Reloncavi fjord, Chile

M. I. Castillo et al.

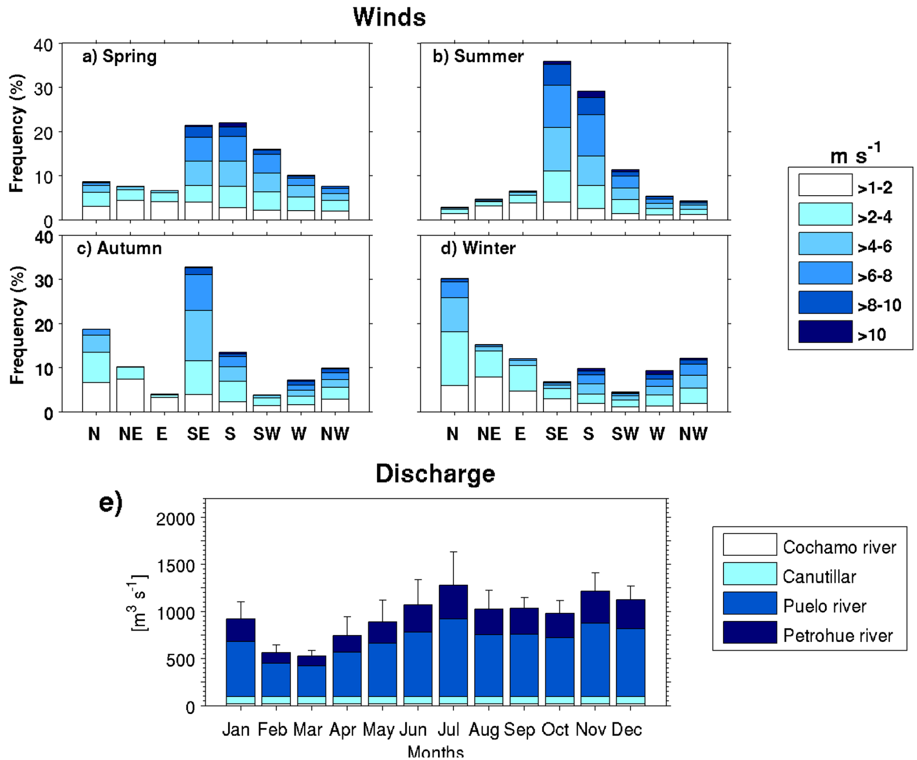

Figure 2. Seasonal variability of the wind vector in the Reloncavi fjord during the period June 2008 to March 2011. The wind-rose indicated the frequency of direction and magnitude for each season **(a)** spring, **(b)** summer, **(c)** autumn and **(d)** winter.

OSD
12, 2535–2564, 2015

Seasonal hydrography in the Reloncavi fjord, Chile

M. I. Castillo et al.

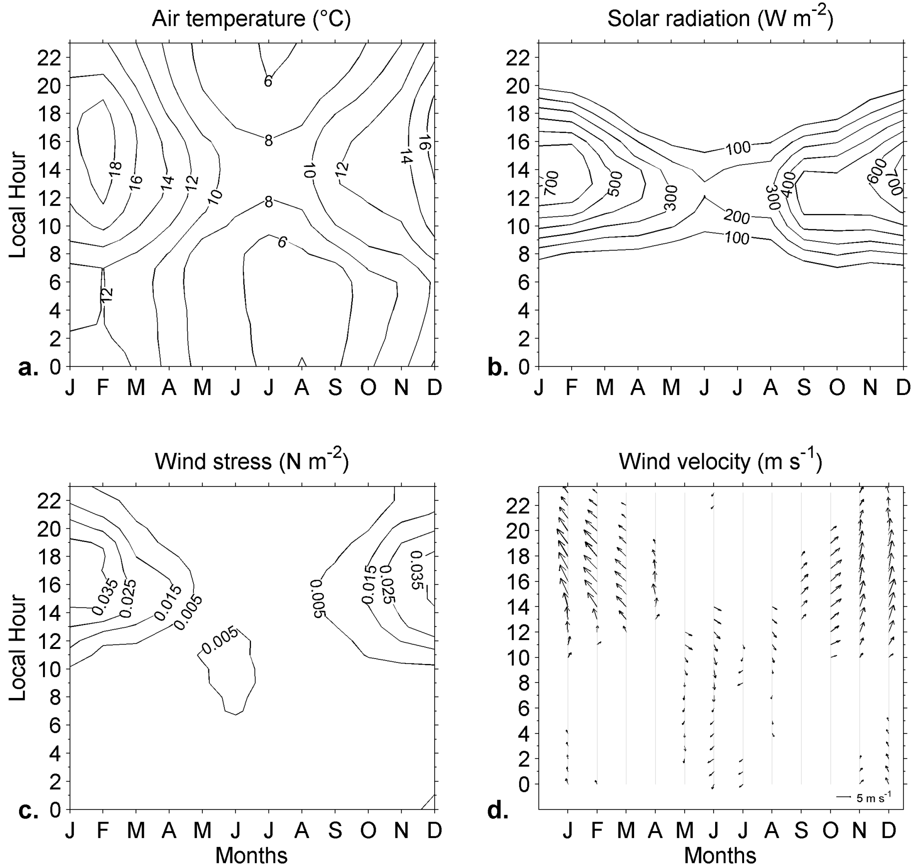

Figure 3. Seasonal variability of the daily cycle of the meteorological variables: **(a)** air temperature, **(b)** solar radiation, **(c)** wind stress magnitude and **(d)** wind velocity (meteorological convention). The *y* axis is the local hour to be consistent with the day-light hours.

OSD
12, 2535–2564, 2015

Seasonal hydrography in the Reloncavi fjord, Chile

M. I. Castillo et al.

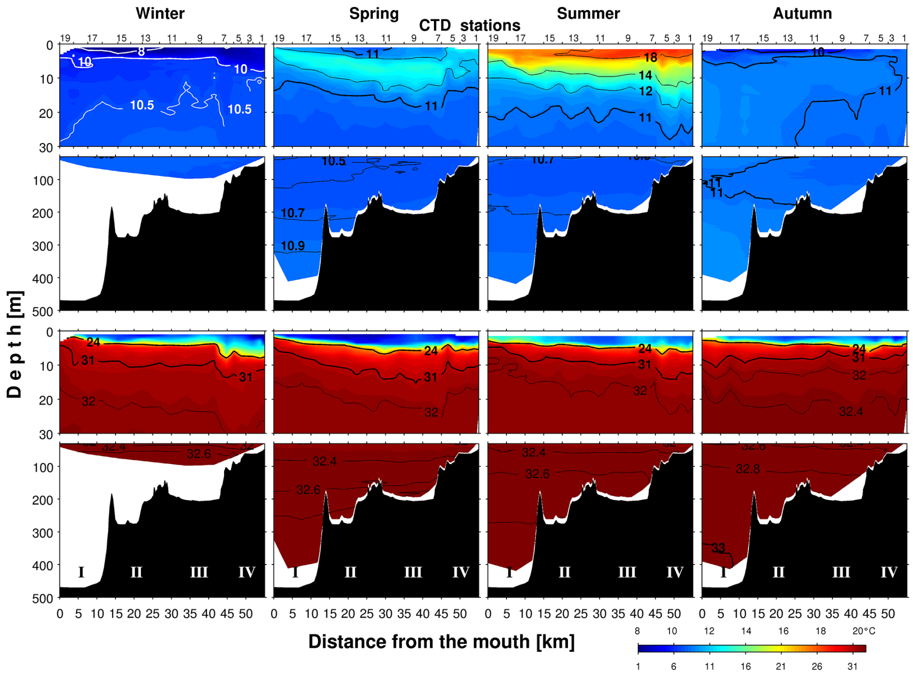

Figure 4. Along-fjord seasonal distribution of Temperature (above) and Salinity (below) for winter, spring, summer and autumn. The figure includes the CTD station number in the top of each panel, and the sub-basins numbers below.

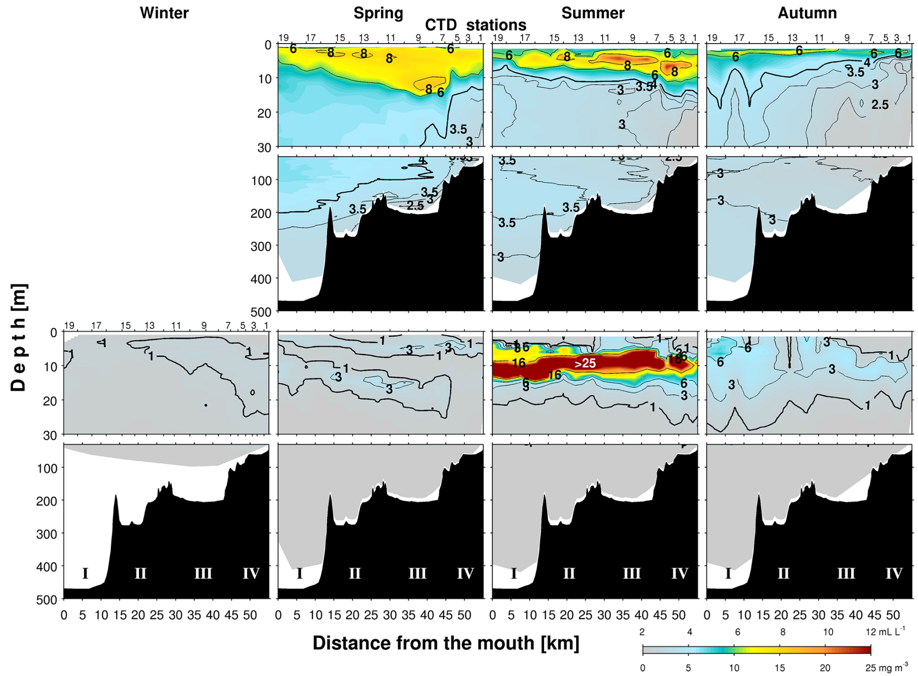

Figure 5. Along-fjord seasonal distribution of Dissolved Oxygen (above) and Chlorophyll (below) for winter, spring, summer and autumn. The figure includes the CTD station number in the top of each panel, and the sub-basins numbers below. There is not DO measurements during winter.

OSD

12, 2535–2564, 2015

Seasonal hydrography in the Reloncavi fjord, Chile

M. I. Castillo et al.

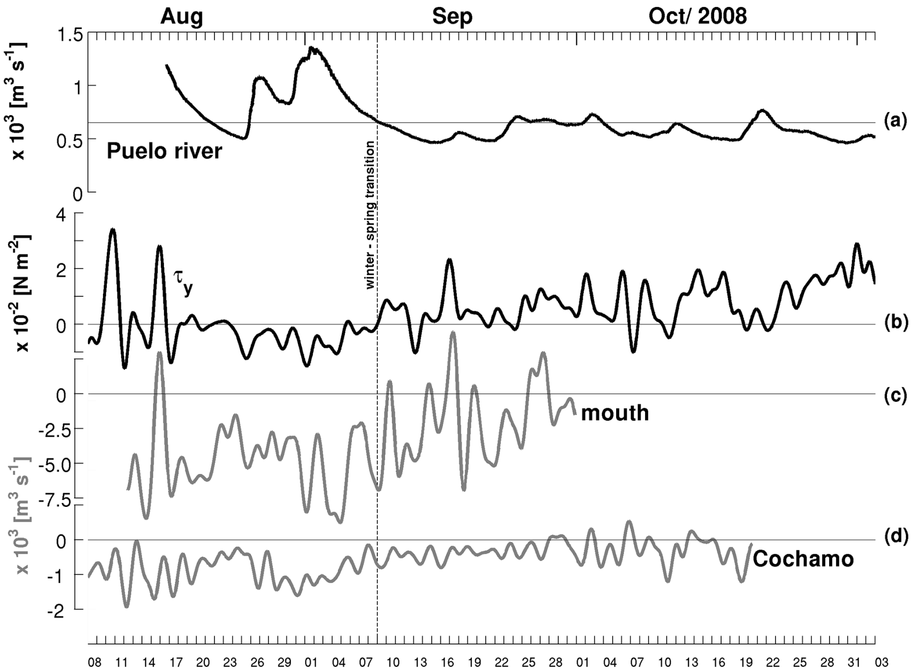

Figure 6. Low-frequency time series of the Puelo river **(a)**, along-fjord wind stress **(b)**, and the volume flux of the upper layer at the mouth **(c)** and at Cochamo **(d)**. Notice the existence of a different scale for the volume flux at each location. The segmented line indicates the seasonal shift in the pattern of winds between late winter to early spring.

OSD
12, 2535–2564, 2015

Seasonal hydrography in the Reloncavi fjord, Chile

M. I. Castillo et al.

Title Page
Abstract | Introduction
Conclusions | References
Tables | Figures
Back | Close
Full Screen / Esc
Printer-friendly Version
Interactive Discussion

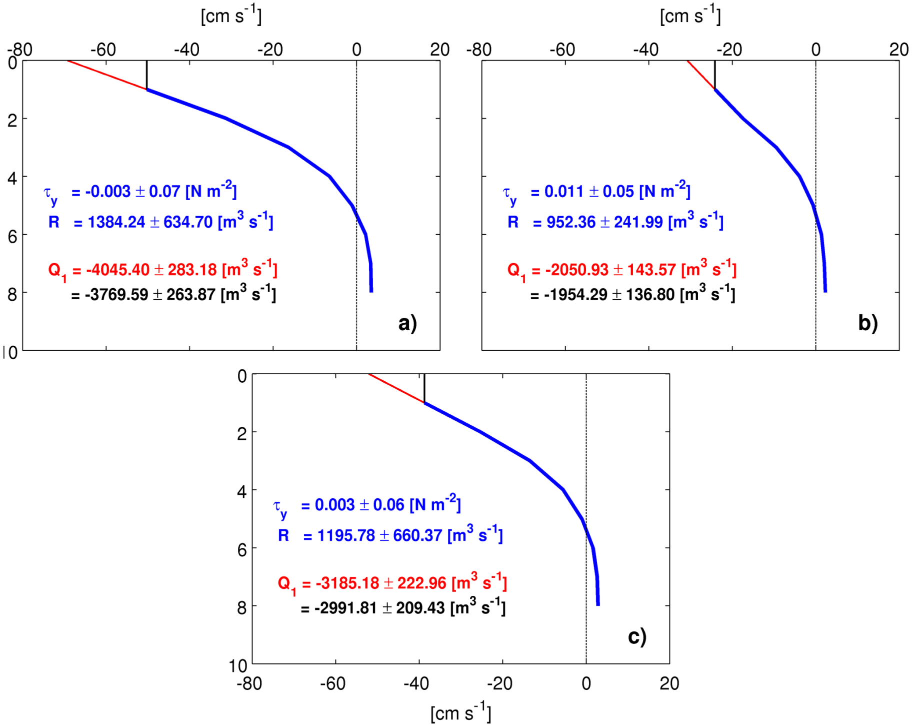

Figure 7. Mean profiles of along-fjord currents (v) at the mouth for the periods of winter **(a)**, spring **(b)** and for the entire period of measurement showed on Fig. 6. The blue line indicates the observed mean which lack in the near surface. The red and black lines indicates two different extrapolations to the surface: linear (red) and nearest (blue) the mean volume flux (Q_1) obtained by the use of both extrapolations are included. Additionally, the average of τ_y for each period and the discharge (R) has been included.

OSD

12, 2535–2564, 2015

Seasonal hydrography in the Reloncavi fjord, Chile

M. I. Castillo et al.

Title Page
Abstract | Introduction
Conclusions | References
Tables | Figures
◀I | ▶I
◀ | ▶
Back | Close
Full Screen / Esc
Printer-friendly Version
Interactive Discussion